RSC Advances

PAPER

View Article Online
View Journal | View Issue

Cite this: *RSC Adv.*, 2022, **12**, 3646

The features of the crystal structure of the layered series hydrates of uridine-5′-monophosphate salts ($UMPNa_x \cdot yH_2O$)†

Pengpeng Yang,[a] Kun Dai,[a] Chenguang Lin,[a] Pengfei Jiao,[c] Fengxia Zou,*[ab] Gulin Zhao*[a] and Hanjie Ying[ac]

Almost all reported salts of nucleotides crystallized from solutions are in the form of hydrate. Layered hydrates often occur in crystals with more than five water molecules per host molecule. In the present report, five single-crystal structures of uridine-5′-monophosphate (UMP) series hydrates of acid or salts ($UMPNa_x \cdot yH_2O$, $x = 0–2$) were determined and analysed. It was found that all crystal hydrates were orthorhombic with a $C222_1$ space group but with mere variation in the plane angle of adjacent bases and the distance between phosphate arms. The packing arrangements of $UMPNa_x \cdot yH_2O$ hydrates present typical layered sandwich structures and show that the UMP molecular layers alternate with water molecular layers parallel to the *ac* plane, linked by hydrogen bonds or coupled with coordinate bonds besides ionic electrostatic interaction. Metal ions were located in water molecular layers as a form of hydration. In addition, we tried to deduce and give insights into the formation of $UMPNa_x \cdot yH_2O$ hydrates. The effect of water molecules and metal ions on the crystal structure and stability was investigated. It was found that the coexistence of relatively rigid architectures constructed by host molecules and flexible interlayer regions was a key factor to the formation of these hydrates. Excessive loss of lattice water would give rise to the irreversible collapse of the host structure and loss of ability to recover to the initial state under humidity. Approximately seven crystal-water molecules were the balance point of sodium salt hydrates at room temperature under 43–76% RH conditions. The number of sodium ions in the crystal lattice is positively correlated with their thermal stability.

Received 4th November 2021
Accepted 16th December 2021

DOI: 10.1039/d1ra08091a

rsc.li/rsc-advances

1 Introduction

Water and salts play an important role in the retention of high-order structures of biomolecules.[1] Typical examples are the A–B and B–Z transitions of DNA governed by water activity. Metal ions are involved in the self-assembly process and possess structure-directing properties in the solution ordering of nucleotides.[2]

Based on the CSD database, we noted that almost all reported salts of the nucleotides crystallized from solutions exist in the form of hydrate, which may be ascribed to their ionized phosphate groups and features of structures of themselves. Layered hydrates often occur in crystals with more than five water molecules per host molecule and are common for compounds such as disodium heptahydrate and monosodium nonahydrate of guanosine-5′-monophosphate (GMP),[3] heptahydrate and hendecahydrate of disodium deoxycytidine-5′-phosphate (dCMP),[4,5] and 6.5 hydrates of calcium salt and strontium salt of inosine-5′-monophosphate (IMP).[6] Besides, many structures display the packing preferences of the orthorhombic space group symmetry. For example, a single crystal of disodium adenosine-5′-triphosphate ($ATPNa_2$) was reported, which exists in three forms of hydrates (such as monohydrates, dihydrates and trihydrates) with the orthorhombic $P2_12_12_1$ space group.[7] For adenosine-5′-monophosphate (AMP), disodium dodecahydrate and monohydrate are of acid form, while for cytidine-5′-monophosphate (CMP), $CMP \cdot 3H_2O$, $CMPNa_2 \cdot 6.5H_2O$, and $CMPBa \cdot 8.5H_2O$ all exist in an orthorhombic arrangement.[1,8–10] It thus appears that such packing mode of nucleotides is relatively preferential. How could it have various hydrates for the same nucleotide? What are the features of these crystal hydrates at the micro level? What are the effects of water molecules and metal ions on the crystal structure and stability? These are very interesting questions.

[a]*National Engineering Technique Research Center for Biotechnology, State Key Laboratory of Materials-Oriented Chemical Engineering, College of Biotechnology and Pharmaceutical Engineering, Jiangsu Synergetic Innovation Center for Advanced Bio-Manufacture, Nanjing Tech University, Nanjing, Jiangsu, 211800, People's Republic of China. E-mail: somnus0715@ntu.edu.cn; 1149@njtech.edu.cn*

[b]*Chemistry and Chemical Engineering, Nantong University, People's Republic of China*

[c]*College of Life Science and Agriculture Engineering, Nanyang Normal University, People's Republic of China*

† Electronic supplementary information (ESI) available. CCDC $UMPH_2 \cdot 5.5H_2O$ (1052110), $UMPNa_{1.0} \cdot 8.5H_2O$ (1051744), $UMPNa_{1.5} \cdot 9H_2O$ (1418433), $UMPNa_2 \cdot 7H_2O$ (1051761), $UMPBa_{8.9}$ H_2O (BAURIP). For ESI and crystallographic data in CIF or other electronic format see DOI: 10.1039/d1ra08091a

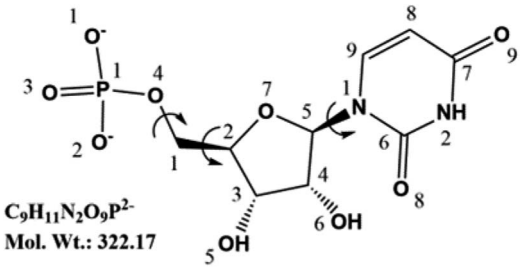

Fig. 1 Structure of UMP^{2-} with atomic numbering. Flexible torsion angles are indicated by φ_1 (C9–N1–C5–O7), φ_2 (C3–C2–C1–O4), and φ_3 (C2–C1–O4–P1).

Uridine-5′-monophosphate (UMP), a representative of nucleotide, as shown in Fig. 1, was used as a monomer in RNA.[11] The UMP sodium salt was employed as an important pharmaceutical intermediate, and was one of the most important antiviral and anti-tumor drugs.[12] It is also an important functional food additive that improves the immune function of organisms and prevents Alzheimer's disease.[13] The structures of barium salt and one of sodium salts have been reported as a form of hydrate with an orthorhombic packing architecture.[14,15] In the present study, we obtained several hydrates. Here, taking uridine-5′-monophosphate (UMP) as an example, we attempted to investigate their structural characteristics, the effect of water molecules and metal ions on crystal stability, the origin of existence and diversity of nucleotide hydrates, and the relationship of water molecules, metal ions, and host molecules in the crystal lattice with hydrate properties.

2 Experimental

2.1 Materials

The raw material for UMP disodium salt powder (CAS number: 3387-36-8, calculated purity > 99% as anhydrous state) was purchased from Biotogether (Nanjing, China) and used after recrystallization. Organic solvents of analytical grade were purchased from commercial sources and used without further purification. Ultrapure water (ELGA PURELABE Classic 18.2 MΩ cm) was used in all the experiments.

2.2 Preparation of UMP series hydrates

The solvent, temperature and pH were taken into consideration as the major factors for screening various $UMPNa_x{\cdot}yH_2O$ hydrates. Single crystals of sodium salts and acid forms of UMP were grown from pure water or water-organic solvent solutions by slow evaporation or slow cooling over a period of several weeks, at a temperature ranging from 4 to 40 °C and a pH ranging from 2 to 9. The organic solvents used in experiments include methanol, ethanol, 1-propanol, 2-propanol, acetone, dimethyl sulfoxide, *N*,*N*-dimethylacetamide, tetrahydrofuran, and acetonitrile. The pK_a values of UMP in aqueous solutions were 1.0 and 6.4 for the dissociation of the phosphate group, and 10.06 for the pyrimidine base. Based on the Henderson–Hasselbalch theory, the ion species distribution of UMP in aqueous solutions can be calculated, as shown in Fig. 2.

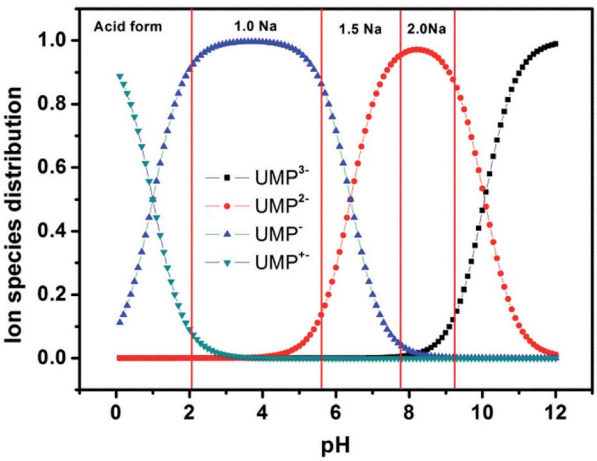

Fig. 2 Plot of the ion species distribution of UMP *vs.* pH in an aqueous solution. The four regions between red lines mean that where different sodium salts or acid forms of UMP hydrates may occur.

Therefore, the crystal forms of different contents of sodium ions may be expected to be obtained by adjusting the original pH of the UMP solution before single-crystal cultivation. In order to ensure the amount of sodium ions that produce crystals, sodium acetate can be considered. Specifically, the single crystal of $UMPH_2{\cdot}5.5H_2O$ was cultured by cooling crystallization of pure water at pH 0.8, as well as $UMPNa_1{\cdot}8.5H_2O$ was obtained from a water–*n*-propyl alcohol solution (1 : 0.5 v/v) at pH 4.0, yet $UMPNa_{1.5}{\cdot}9H_2O$ was cultured by evaporation crystallization of a water–DMSO solution (1 : 0.8 v/v) at pH 7.0 and room temperature, while $UMPNa_2{\cdot}7.0H_2O$ was obtained by cooling crystallization of a water–ethanol solution (1 : 0.3 v/v) at pH 8.5 and 1% sodium acetate. The pH was adjusted using an aqueous solution of 0.05 M HCl or 0.05 M NaOH.

2.3 Single-crystal X-ray diffraction

The single-crystal X-ray diffraction data for $UMPNa_x{\cdot}yH_2O$ hydrates were collected using a Bruker APEX-II CCD diffractometer with Mo Kα radiation (graphite monochromator, λ = 0.71073 Å). The structures were solved by a direct method and refined by full-matrix least-squares on F^2 for all data using a SHELX-2018 (Sheldrick, 2008). Atomic displacement parameters were refined for all non-hydrogen atoms. The hydrogen atoms were placed in calculated positions. The disordered oxygen atoms of water molecules and disordered sodium ions were treated as a pair of split atoms. The Materials Studio 6.0 and Mercury 3.3 software[16] were used for crystal structure analysis and visualization based on crystal structure data.

2.4 Determination of water content in lattices

A gravimetric method, as a quick and simple approach to determine the water content of $UMPNa_x{\cdot}yH_2O$ hydrates, is available and suitable for rough measurement. Solid powders were subjected to 110 °C heat in an oven and maintained for about three hours until constant weight was achieved. The loss of water can be calculated from the variation in weight. Accurate

determination of water content was carried out by the Karl Fischer method (Metrohm 870 KF Titrino plus, Switzerland).

2.5 Determination of sodium ion contents

The sodium ion content of $UMPNa_x \cdot yH_2O$ hydrates was measured by single X-ray diffraction with a sodium ion-selective electrode using an auto-potentiometric titrator (Metrohm 848 Titrino plus, Switzerland). A Ag/AgCl electrode (Metrohm 6.0726.100) filled with 3 mol L^{-1} KCI was used as the reference electrode for the determination of sodium ions.

2.6 Powder X-ray diffraction (PXRD)

Powder X-ray diffraction was performed using a Bruker D4 diffractometer with Cu Kα1 radiation (λ = 1.54178 Å). The voltage and current were 40 kV and 100 mA, respectively. Samples were scanned in the reflection mode over a 2-theta range of 2–60°, with a step size of 0.02°. Data were acquired at ambient temperature. To prevent the atmospheric humidity effect, the necessary samples were covered during the analysis with a 10 μm polyethylene film.

2.7 Thermal analysis (DSC/TG)

Thermogravimetric (TG) and differential scanning calorimetry (DSC) were carried out simultaneously using a Netzsch STA-409 system. Accurately weighed samples (approximately 5 mg) were placed in an aluminum crucible and heated at a constant heating rate of 10 °C min^{-1} in the temperature range of 40–400 °C under the flow of nitrogen at a rate of 20 mL min^{-1}. The instrument was calibrated using indium as the reference material.

2.8 Energy calculation

The potential energy calculation (at 0 K under absolute vacuum) of single UMP species in various crystal lattices of $UMPNa_x \cdot yH_2O$ hydrates was performed by Dmol^3 based on DFT (density functional theory) with a DNP basis set, PBE functional, SCF tolerance 1.0×10^{-6}, smearing (0.005 Ha), fine integration grid, thermal 0.0050 occupation, and a global orbital cutoff of 4.2 angstrom.[17–19] Hydrogen atom positions of every UMP species were first optimized by Dmol^3 performed using the Materials Studio 6.0 software. The potential energy gap between any two single UMP species was described as $\Delta E = E_i - E_0$ (E_i is the potential energy of the single UMP species in the crystal lattice of various $UMPNa_x \cdot yH_2O$, and E_0 is that of $UMPNa_2 \cdot 7.0H_2O$). Herein, we take the $UMPNa_2 \cdot 7.0H_2O$ hydrate as a reference.

3 Results and discussion

3.1 Crystal structure analysis of $UMPNa_x \cdot yH_2O$ hydrates

We performed some screening and successfully obtained a series of single-crystal structures of $UMPNa_x \cdot yH_2O$ hydrates. In terms of a simplified molecular formula based on water molecules per UMP molecule, there were 5.5 water molecules for the acid form (one of water oxygen (O12), which was located in a 2-fold rotation axis; see Fig. S1†), 8.5 for monosodium salt, 9.0 for one and a half sodium salts (one of sodium ions was shared by two UMP species in an asymmetry unit cell; see Fig. S2†), and 7.0 for disodium salts, as listed in Table 1. It was found that they were non-stoichiometric due to non-localized water molecules. Interestingly, all these UMP hydrates were shown as orthorhombic with a $C222_1$ space group and the cell parameters were quite close. They were isostructural hydrates, and of isomorphism.[20] There was no significant regularity about

Table 1 Crystallographic data of UMP series hydrates and the conformation of their single molecules[a]

Items	1	2	3	4	5*
Simplified formula	$UMPH_2 \cdot 5.5H_2O$	$UMPNa_{1.0} \cdot 8.5H_2O$	$UMPNa_{1.5} \cdot 9H_2O$	$UMPNa_2 \cdot 7H_2O$	$UMPBa \cdot 8.9H_2O$
Formula weight (g mol^{-1})	846.54	968.36	1001.31	480.15	501.57
a [Å]	8.9160(18)	8.924(3)	8.917(3)	8.9287(13)	21.11
b	22.953(5)	22.990(1)	22.854(9)	22.941(3)	9.06
c	19.545(4)	19.456(8)	19.353(7)	19.433(3)	20.98
V [$Å^{-3}$]	3999.9(14)	3992(3)	3944(2)	3980.5(10)	4012.56
Crystal system	Orthorhombic	Orthorhombic	Orthorhombic	Orthorhombic	Orthorhombic
Space group H–M	$C222_1$ (no. 20)	$C222_1$ (no. 20)	$C222_1$ (no. 20)	$C222_1$ (no. 20)	$C222_1$ (no. 20)
Space group Hall	$C2c2$	$C2c2$	$C2c2$	$C2c2$	$C2c2$
Z	4	4	4	8	8
D(calc) [g cm^{-3}]	1.406	1.611	1.686	1.602	2.052
Mu(Mo Kα) [mm]	0.208	0.250	0.267	0.264	
F(000)	1784	1984	2036	1952	
Crystal size [mm]	0.10 × 0.20 × 0.30	0.22 × 0.25 × 0.26	0.22 × 0.26 × 0.28	0.19 × 0.24 × 0.26	
Temperature (K)	293	296	296	296	
Theta min–max [deg]	1.8, 25.4	1.8, 25.0	2.1, 25.0	1.8, 25.0	
Tot., uniq. data, R(int)	3677, 3677, 0.091	10 082, 3468, 0.033	14 320, 3473, 0.040	10 733, 3496, 0.030	
Observed data [I > 2.0 sigma(I)]	2386	3188	3329	3365	
N_{ref}, N_{par}	3677, 234	3468, 286	3473, 335	3496, 317	
R, wR_2, S	0.0900, 0.2354, 1.12	0.1269, 0.3564, 1.85	0.1186, 0.3481, 1.98	0.1077, 0.3146, 1.73	0.098
CCDC no.	1052110	1051744	1418433	1051761	BAURIP

[a] "*" indicates reported data.

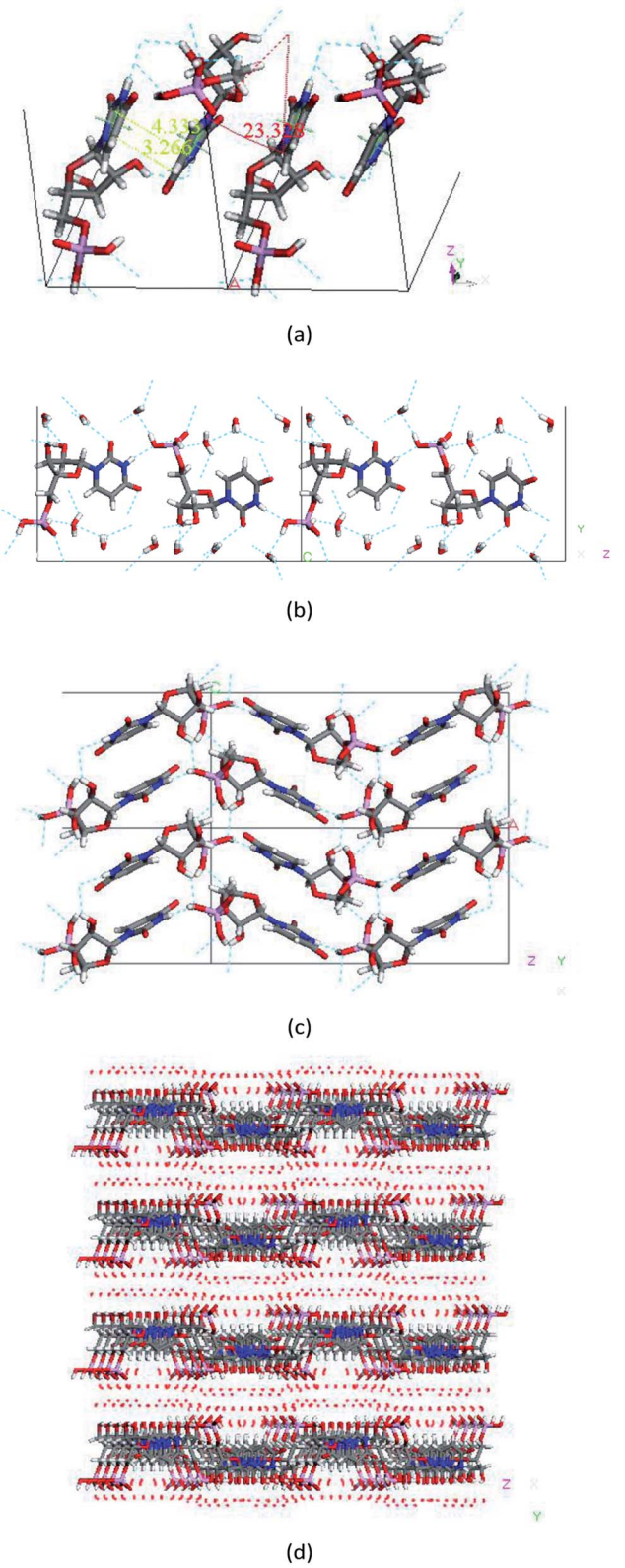

Fig. 3 (a) Molecular columns along the *a*-axis; (b) molecular chains along the *c*-axis; (c) molecular layers running parallel to the *ac* plane; and (d) layered packing structures of the hydrate of $UMPNa_x \cdot yH_2O$ ($x = 0$; $y = 5.5$ as an example), where the red atoms are oxygen atoms of water and its hydrogen atoms are omitted for clarity.

the dependence of the cell volume on the content of crystal water and sodium ions. Partial water molecules and sodium ions existed in distorted ways in the crystal lattices of $UMPNa_x \cdot yH_2O$, and a further declaration of order/disorder was made in Table S1.†

3.2 Structural features of $UMPNa_x \cdot yH_2O$

For all hydrates, the base moieties of UMP were partially overlapped and stacked with a spacing of approximately 3.02 to 4.54 Å to form a columnar structure along the *a*-axis by base-stacking forces. The orientation of neighbouring molecules along the *a*-axis was opposite, and the included angle of base planes of two adjacent UMP molecules was about 4.70° to 27.91° (see Fig. 3a and 4b). In the *c*-axis direction, the UMP molecules interact mainly *via* hydrogen bond interactions (dominated by the bond between N–H and P–O of the other one), accumulating as chains running parallel to the *c*-axis with water molecules and sodium ions situated between the chains. Water-intermediated hydrogen bonds exist around the chains (see Fig. 3b).

As a result, the molecular layers running parallel to the *ac* plane were constructed and sustained by alternating hydrogen bonds and base stacking interactions (Fig. 3c), which laid the foundation for the crystal structural stability. What is more, between two such layers, a region or cavity was produced and used to accommodate guest molecules. On the whole, the packing arrangement of the UMP hydrate presents sandwich structures and shows that the UMP molecular layers alternate with water molecular layers parallel to the *ac* plane, linked by hydrogen bonds or coupled with coordinate bonds. The typical packing arrangements are shown in Fig. 3d.

From Fig. 3d, $UMP \cdot 5.5H_2O$ was a typical layered hydrate with the layered packing feature. What is more, although sodium ions or barium ions were introduced and incorporated into the crystal lattice, such packing architecture was no significant change, but accommodated the blue region (Fig. 4a; the distribution of sodium ions in the crystal lattice of UMP various hydrates is shown in Fig. S3†) in the form of hydration, formed by the alternating phosphate arms and vertical bases in the opposite direction within two host layers. The structural features of the reported crystal structure of UMP barium salt are in accordance with that of $UMPNa_x \cdot yH_2O$; they were isomorphous structures. Yet an exception was the crystal structure of potassium uridine-5′-monophosphate salts (UMPK).[21] From Fig. S6,† the coordination of Na gives priority to Na–O (water) for the $UMPNa_x \cdot yH_2O$ hydrates, and the oxygen of water contributes mainly to the coordination sphere of Na ions, and there is not the case that two UMP^{2-} moieties located in two adjacent layers were linked by the sodium ion coordination interaction. Sodium ions somewhat resemble a ship anchored to the shore (host molecular layer), with flexibility to some extent. In contrast to the structures of UMPNa hydrates, despite an orthorhombic $P2_12_12_1$ space group for UMPK, UMPK does not create a layered architecture but a rather compact and more uniform structure in all dimensions with a density of 1.76 g cm^{-3} at 300 K, while that of UMPNa oscillates around 1.65 g cm^{-3}. Further analyses of the crystal structure of UMPK

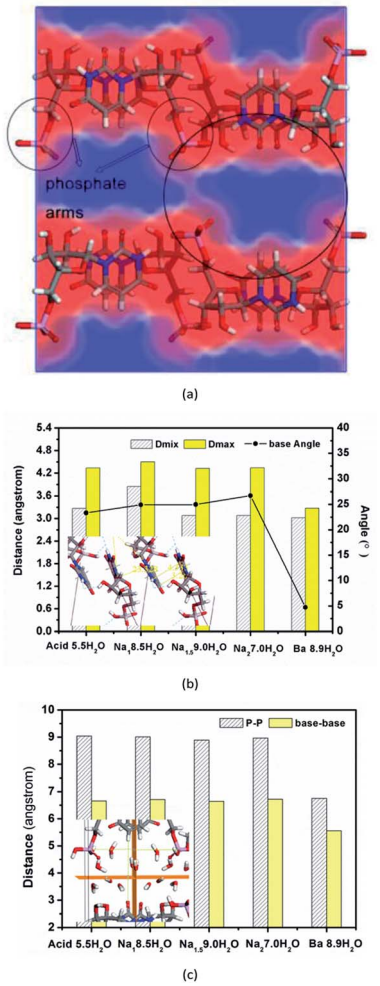

Fig. 4 (a) Local flexible space in UMPNa$_x$·yH$_2$O hydrates; (b) distances and angles between base planes of two adjacent UMP molecules, D_{max} and D_{min} indicating the maximum and minimum distances; and (c) the distances between two adjacent phosphate arms (P–P), and between two bases (base–base) of UMP molecules. Auxiliary planes were added for the vertical distance measurement.

found that the potassium cation is seven-coordinated (see Fig. S4 and S5†), making the angle of adjacent two uracil base planes enlarged a lot, which weakens the interaction of base fragments. The potassium ion was bound by almost all the available O atoms of the counterion, which forms strong electrostatic interactions between K and O atoms, stabilizing predominantly the crystal structure of UMPK, which was different remarkably from the UMPNa hydrates. The electrostatic interactions caused by sodium ions and UMP anions were not the key factor for sustaining the host architecture of UMP sodium salt hydrates, which can be supported by the coordination effect of the sodium ion (details are shown in Fig. S6†) and its disordered existence state.

3.3 Conformation characteristics of single UMP molecules in crystal lattices of UMPNa$_x$·yH$_2$O

As for the conformation of single UMP molecules in crystal lattices, it was found that the orientation of the uracil base relative to the sugar was anti and the base existed in the keto form for all UMPNa$_x$·yH$_2$O series hydrates. All the furanose ring conformation was C(4)-endo (based on the plane defined by C5–O7–C2), and C3 was nearly on such plane. The phosphate moieties of hydrates of mono-/sesqui-sodium salts and its acid form existed as complete or partial protonated species, apart from that of disodium salts. For the single UMP molecule in many of crystal lattices, the torsion φ_1 was from 42.7 to 45.9°, φ_2 from 49.6 to 57.5°, and φ_3 from 176.0 to 179.7°. Yet for the structure of anhydrous potassium salt, the conformation of UMP species changes a lot, with merely 20.3° of the torsion of φ_1 (C9–N1–C5–O7). Nevertheless, in spite of the variation in these group moieties or torsions, the energy of single UMP species in the crystal lattice of all the hydrates was quite close, where their energy gap was merely from −3.25 to 12.80 kJ mol^{-1} (see Table 2).

3.4 Features of the local space

Herein, the local space was referring to the region or cavity between two host molecular layers, as shown in Fig. 4a. It was found that there was difference in the distances and angles between base planes of two adjacent UMP molecules along the a-axis direction for various UMPNa$_x$·yH$_2$O hydrates, but no strict regularity with the change in the number of sodium ions and water molecules, as shown in Fig. 4b. There is difference in the size of local space of the water layer along the b-axis in sandwich layered crystal structures as well, but this does not strictly depend on the number of sodium ions and water molecules, as shown in Fig. 4c. This indicates that the local cavity constructed by phosphate arms and base pairs of adjacent UMP molecules along the b-axis and c-axis was so flexible, which accommodated different amounts of water molecules and metal ions *via* some adjustment of its own structure. Such rather structural flexibility endowed by particular structural features was analogous to the adaptive mechanism, addressing the surrounding changes without changing the inherent orthorhombic host packing mode. Yet it should be pointed out that barium ion could shorten the distance between phosphate

Table 2 Torsional angles and conformational energy of UMP series hydrates[a]

Items	1	2	3	4	5*
Torsions φ_1, φ_2, φ_3, (°)	45.9, 52.0, 179.7	43.2, 54.6, 179.7	43.9, 57.2, 177.7	42.7, 56.0, 178.9	43.3, 55.2, 176.0
ΔE (kJ mol^{-1})	−3.25	7.01	7.35	0.00	12.80

[a] "*" indicates reported data.

arms from 9.0 to 6.5 Å averagely, narrow the distance between the adjacent base planes from 3.02 to 4.54 Å averagely along the *a*-axis, and reduce the size of the local space of the water layer, which may be ascribed to its stronger electrostatic action than that of mono-valent sodium ions.

In addition, the existence of metal ions and water molecules can compel the angle of base planes and the conformation of single UMP molecules to make some adjustment (see Fig. 4), but the relative weak interaction with host molecules was not enough to change the original packing mode, which was confirmed by the mobility of water or sodium ions in the crystal lattice. As a result, various $UMPNa_x \cdot yH_2O$ hydrates have the same molecular arrangement. Actually, similar structures were observed in the crystals of $IMPNa_2$, $CMPNa_2$, and $GMPNa_2$.[22,23]

3.5 Discussion of the formation of $UMPNa_x \cdot yH_2O$ hydrates

In this work, we tried to deduce the origin of the formation of different hydrates. The affinity of the phosphate group and ribose moiety of the UMP molecule to the water molecule was so strong that UMP exists as a hydration form in aqueous solutions. When supersaturation was introduced into the crystallization system, the well-organized aggregation would occur among the hydrous UMP ions and induce nucleation. Water molecules behave as a "bridge" or "glue" among host molecules, and their participation can reduce the free energy during solute molecule aggregation.[24–26] The orthorhombic packing mode was efficient for the molecular assembly of these kind of compounds. On the basis of such mode, the voids or cavities with the orientation parallel to the base plane could be generated between UMP molecules (see Fig. 4a). Both the distance of phosphate arms between two neighbouring UMP molecules down the *c*-axis and that of bases down the *b*-axis mostly contribute to the size of such space. It was capable of accommodating water molecules or hydrated metal ions. When hydrous UMP species from bulk solution, as a growth unit, were close to the combination site of the solvated crystal face and proceeded to combination, those water molecules around the cavities could be retained, while those outside the cavities tended to be extruded. Thus, it led to the formation of UMP hydrates.

However, the conformation of a molecule was mainly dependent on the thermodynamic conditions of a system, and the most preferential and stable conformer varied with the solvent environment, temperature, and pH. Under the same packing mode, therefore, it was possible to result in various cavities of different sizes as well, especially for the nucleotide molecule with high molecular flexibility, which was related to how many water molecules were accommodated. However, it is not the only factor. From Fig. 4c, no preferable regularity was observed between the cavity size and crystal water number. In fact, apart from such space size, the water density of this region may be another reason, and it was reflected in the crystal density to some extent. Obviously, the existence of metal ions narrowed the distance of phosphate arms due to the electrostatic interaction, especially for bivalent barium ions, increased the water density of local regions, and thus, they make it possible to accommodate more water molecules under similar sizes of cavities.

3.6 Behaviours of lattice water mediated by humidity and the relationship with the crystal structure

We also investigated the desorption/adsorption behaviour of lattice water for series hydrates of UMP sodium salts by humidity cycle experiments at room temperature. Each crystalline powder ($UMPNa_1 \cdot 8.5H_2O$, $UMPNa_1.5 \cdot 9H_2O$ and $UMPNa_2 \cdot 7H_2O$) was put into an absolute dry environment produced by P_2O_5 powder initially for several days until the weight became constant. Then, they were transferred to 43%, 58% and 76% of relative humidity conditions respectively for several days created by different saturated inorganic salt solutions (Greenspan, 1977) until the weight ceased to change and attained a new equilibrium. The sample weight in two stages was recorded at regular intervals and used for tracing the water content variation. The accurate value of sample water content was measured by the Karl Fischer method (Metrohm 870 KF Titrino plus, Switzerland).

It was found that most of the water molecules in the crystal lattice for three hydrates would be lost rapidly under 0% RH, and the crystal structures would make gradual adjustment and rearrangement along with the desorption of lattice water. Yet the water in lattices was hard to complete desorption despite a duration time of more than two weeks, and the original crystalline powders were transformed into the corresponding lower hydrates. When dehydrated samples were transferred and subjected to some humidity environments, they exhibited the potential to absorb the gaseous water molecule from surroundings, with embedded into the crystal lattice, and recovered the original packing architecture, which resembled a sponge squeezed out for reabsorbing water. The uptake rate of water for the dehydrated sample increases remarkably with relative humidity rising in surroundings, and the time reaching a new balance would shorten.

Yet interestingly, regardless of the number of sodium ions or water molecules in crystal lattices, all these tested hydrates were transferred to approximately seven crystal-water molecules of solid powder with 26.0 ± 1.0% of water content, where data fluctuation was influenced by the content of sodium ions. In other words, those hydrates were greater than seven crystal-water molecules per UMP species that have a tendency to lose partial water, while those lower hydrates with less than seven to absorb gaseous water molecules from surroundings. There exists a balance region of about seven lattice-water molecules at room temperature under 43–76% RH conditions for UMP sodium salt hydrates (see Table S2†). It indicated that the uptake capacity of UMP salts to water molecules was mainly dominated by the relatively rigid skeleton structure constructed by host molecules, and the metal ion effect was secondary.

Fig. 5 shows the desorption/adsorption behaviour of seven disodium hydrates of UMP and the structure evolution was at three key points ①–③, as captured by powder X-ray diffraction (PXRD) analysis. When a new equilibrium was attained, the solid powder recovered to the initial phase. It was different from

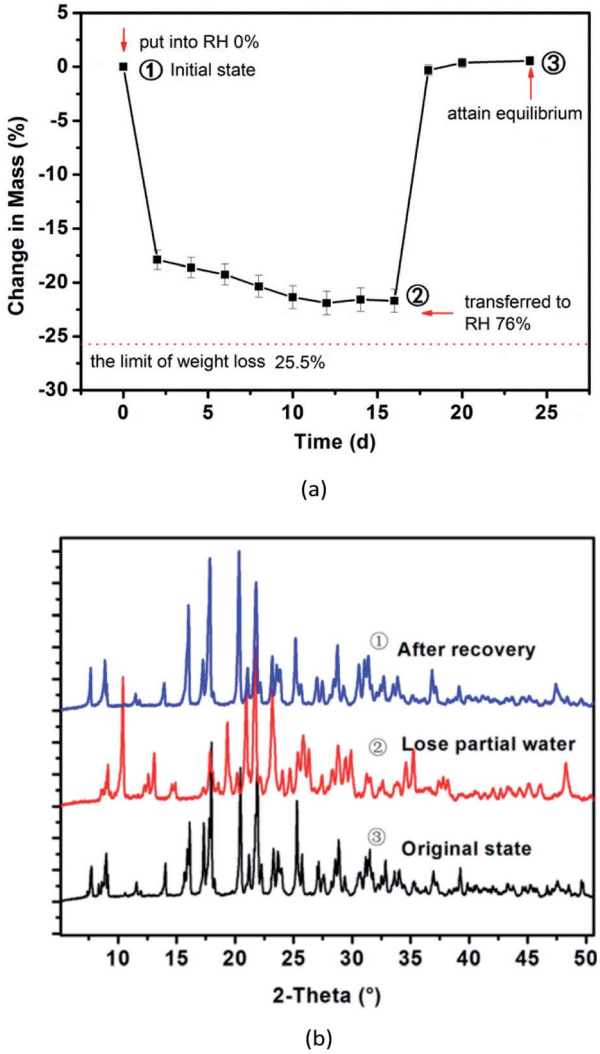

Fig. 5 Desorption/adsorption profiles of lattice water of $UMPNa_2 \cdot 7H_2O$ hydrate (a) and evolution of its structure by PXRD (b) UMP.

adenosine 3′,5′-cyclic monophosphate sodium methanol trihydrate,[27] and the solid powders of UMP sodium salt would retain high crystallinity after losing partial water and effectively avoiding the collapse of the structure. It is worth noting that such a recovery capability would be disabled when the structures are destroyed, brough about by excessive loss of lattice water, such as with treatment with a high temperature (after being subjected to 110 °C for 2 h, the degree of crystallinity was reduced dramatically and no more than 12% water could be adsorbed).

Table 3 Effect of the sodium ion number in UMP hydrates on their thermal stability

Sample	Sodium ion number	Initial melting point (°C)	Starting point of carbonization (°C)
$UMPH_2 \cdot 5.5H_2O$	0	180 °C	—
$UMPNa_{1.0} \cdot 8.5H_2O$	1.0	216 °C	220 °C
$UMPNa_{1.5} \cdot 9.0H_2O$	1.5	224 °C	224 °C
$UMPNa_2 \cdot 7.0H_2O$	2.0	Not detected	230 °C

3.7 Effect of the sodium ion number on the thermal stability of UMP hydrates

The stability of UMP series hydrates ($UMPNa_x \cdot yH_2O$, $x = 0$, 1.0, 1.5 and 2.0) against heat was investigated by a hot-stage microscope experiment from room temperature to 250 °C at 5 °C min^{-1} heating program. The initial melting point and starting point of carbonization were recorded. Herein, the latter referred to the temperature point from transparent or white to yellow and opacity for tested solid samples. The results are given in Table 3.

It was found that both the initial melting point and starting point carbonization for $UMPNa_x \cdot yH_2O$ increased markedly as the amount of sodium ions in lattice increased. There is an obvious melting phenomenon for $UMPNa_{1.0} \cdot 8.5H_2O$ and $UMPNa_{1.5} \cdot 9.0H_2O$. Yet their melting processes were accompanied by carbonization, while carbonation and decomposition were directly detected without apparent melting for the disodium salt hydrate. Accordingly, the thermal stability of $UMPNa_x \cdot yH_2O$ hydrates increased with the increase in the amount of sodium ions in lattices, which may be ascribed to the change in the Na^+ coordination structure, on the one hand, from the main Na–O (water) coordination mode to Na–O (UMP) interaction type. With the loss of water in lattices, the electrostatic interactions caused by sodium ions and UMP anions were likely to be the main factor retaining the stability of structure. On the other hand, more the ions per asymmetric unit, the stronger would be the cohesive energies of crystals.[28]

3.8 TG-DSC analysis of layered UMP disodium heptahydrate

To further investigate the thermal behaviours of the layered hydrate, the TG-DSC experiment was conducted to characterize UMP disodium heptahydrate at a constant heating rate of 10 °C min^{-1} in the temperature range of 40–400 °C in a nitrogen atmosphere. The result is shown in Fig. 6. It was found that there are two apparent endothermic stage and the peaks were located in 100.2 °C and 133.0 °C, which may be in relation to the host structural adjustment caused by water loss. Yet overall, water in the crystal lattice displays a process of gradual and continuous desorption from 60 to 230 °C. No significant melting occurs before the solid decomposes, as observed form

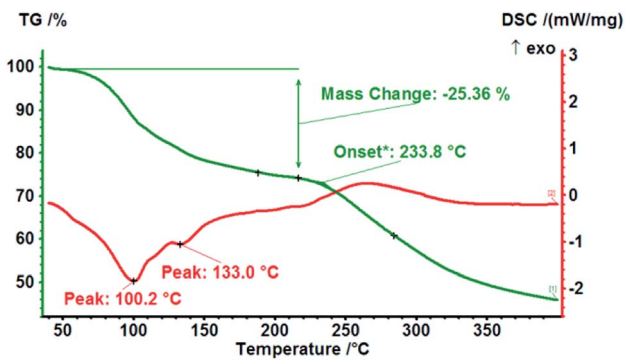

Fig. 6 TG-DSC curves of UMP disodium heptahydrate.

the DSC curve, and the onset of decomposition temperature was 233.8 °C, in agreement with the result of the hot-stage microscope experiment.

4 Conclusions

In this report, the crystal structures of $UMPNa_x{\cdot}yH_2O$ series hydrates were determined and proved to be orthorhombic with a $C222_1$ space group, which presents a typical layered sandwich packing architecture that the UMP molecular layers alternate with water molecular layers. The coexistence of the rigid architecture layers constructed by host molecules and the flexible part of the interlayer region caused by high flexibility of single UMP molecules was the key factor for the formation of various hydrates under different conditions without changing the inherent host packing mode. To some extent, regardless of how many water molecules or metal ions are present in lattices, the local structural adjustment could be made to adapt to the crystallization surrounding change. The size of the local space constructed by phosphate arms did not present strict regularity with the change in the number of sodium ions and water molecules, yet it was influenced by the hydration effect of metal ions in the interlayer local region, especially for divalent barium ions. Approximately seven crystal-water molecules were proved to be the balance point for hydrates of UMP sodium salts at room temperature under 43–76% RH conditions. The thermal stability of $UMPNa_x{\cdot}yH_2O$ hydrates was correlated with the existence of sodium ions, increasing with the increase in the number of sodium ions in lattices. The behaviour of water in the crystal lattice was proved to be a gradual and continuous desorption process when subjected to heating. Excessive loss of lattice water would give rise to the irreversible collapse of the host structure and loss of the ability to recover to the initial state under humidity. These findings contribute to our understanding of the structural features of layered hydrates of nucleotides, the origin of existence and diversity of the nucleotide hydrate, as well as the relationship of water molecules, metal ions, and host molecules in the crystal lattice with hydrate properties.

Conflicts of interest

There are no conflicts to declare.

Acknowledgements

Pengpeng Yang, Fengxia Zou thanked the National Natural Science Foundation of China (NSFC 21908100, 21908114), and Jiangsu Synergetic Innovation Center for Advanced Bio-Manufacture XTE1847.

Notes and references

1 Y. Sugawara, A. Nakamura, Y. Iimura, K. Kobayashi and H. Urabe, *J. Phys. Chem. B*, 2002, **106**, 10363–10368.
2 E. Bouhoutsos-Brown, C. L. Marshall and T. J. Pinnavaia, *J. Am. Chem. Soc.*, 1982, **104**, 6576–6584.
3 M. A. Viswamitra and T. P. Seshadri, *Nature*, 1974, **252**, 176–177.
4 J. Pandit, T. Seshadri and M. Viswamitra, *Acta Crystallogr., Sect. C: Cryst. Struct. Commun.*, 1983, **39**, 342–345.
5 F. A. Perras, I. Korobkov and D. L. Bryce, *Phys. Chem. Chem. Phys.*, 2012, **14**, 4677–4681.
6 E. A. Brown and C. E. Bugg, *Acta Crystallogr., Sect. B: Struct. Crystallogr. Cryst. Chem.*, 1980, **36**, 2597–2604.
7 Y. Sugawara, N. Kamiya, H. Iwasaki, T. Ito and Y. Satow, *J. Am. Chem. Soc.*, 1991, **113**, 5440–5445.
8 Y. Sugawara, H. Urabe, K. Kobayashi, Y. Iimura and H. Iwasaki, *Mol. Cryst. Liq. Cryst. Sci. Technol., Sect. A*, 1996, **277**, 255–258.
9 S. Neidle, W. Kühlbrandt and A. Achari, *Acta Crystallogr., Sect. B: Struct. Crystallogr. Cryst. Chem.*, 1976, **32**, 1850–1855.
10 J. Sherfinski, R. Marsh, A. Chwang and M. Sundaralingam, *Acta Crystallogr., Sect. B: Struct. Crystallogr. Cryst. Chem.*, 1979, **35**, 2141–2144.
11 R. J. Wurtman, M. Cansev, T. Sakamoto and I. H. Ulus, *Annu. Rev. Nutr.*, 2009, **29**, 59–87.
12 J. D. Carver, *J. Nutr.*, 1994, **124**, 144S–148S.
13 T. Tsujinaka, M. Kishibuchi, S. Iijima, M. Yano and M. Monden, *J. Parenter. Enteral Nutr.*, 1999, **23**, S74–S77.
14 T. Seshadri, M. Viswamitra and G. Kartha, *Acta Crystallogr., Sect. B: Struct. Crystallogr. Cryst. Chem.*, 1980, **36**, 925–927.
15 E. t. Shefter and K. Trueblood, *Acta Crystallogr.*, 1965, **18**, 1067–1077.
16 C. F. Macrae, I. J. Bruno, J. A. Chisholm, P. R. Edgington, P. McCabe, E. Pidcock, L. Rodriguez-Monge, R. Taylor, J. Streek and P. A. Wood, *J. Appl. Crystallogr.*, 2008, **41**, 466–470.
17 J. P. Perdew, W. Yang, K. Burke, Z. Yang, E. K. Gross, M. Scheffler, G. E. Scuseria, T. M. Henderson, I. Y. Zhang and A. Ruzsinszky, *Proc. Natl. Acad. Sci. U. S. A.*, 2017, **114**, 2801–2806.
18 B. Delley, *J. Chem. Phys.*, 2000, **113**, 7756–7764.
19 B. Delley, *J. Chem. Phys.*, 1990, **92**, 508–517.
20 S. Ranjan, R. Devarapalli, S. Kundu, S. Saha, S. Deolka, V. R. Vangala and C. M. Reddy, *IUCrJ*, 2020, **7**, 173–183.
21 K. N. Jarzembska, K. Ślepokura, R. Kamiński, M. J. Gutmann, P. M. Dominiak and K. Woźniak, *Acta Crystallogr., Sect. B: Struct. Sci., Cryst. Eng. Mater.*, 2017, **73**, 550–564.
22 M. Sriram, Y. C. Liaw, Y. G. Gao and A. J. Wang, *Acta Crystallogr., Sect. C: Cryst. Struct. Commun.*, 1991, **47**, 507–510.
23 S. Katti, T. Seshadri and M. Viswamitra, *Curr. Sci.*, 1980, 533–535.
24 S. Aitipamula, P. S. Chow and R. B. Tan, *Cryst. Growth Des.*, 2014, **14**, 6557–6569.
25 S. Aitipamula, V. R. Vangala, P. S. Chow and R. B. Tan, *Cryst. Growth Des.*, 2012, **12**, 5858–5863.
26 A. Berzins, E. Skarbulis, T. Rekis and A. Actins, *Cryst. Growth Des.*, 2014, **14**, 2654–2664.
27 P. Yang, C. Lin, W. Zhuang, Q. Wen, F. Zou, J. Zhou, J. Wu and H. Ying, *CrystEngComm*, 2016, **18**, 1699–1704.
28 B. Winter and M. Faubel, *Chem. Rev.*, 2006, **106**, 1176–1211.